J Electr Eng Technol Vol. 9, No. 3: 1119-1124, 2014
http://dx.doi.org/10.5370/JEET.2014.9.3.1119

ISSN(Print) 1975-0102
ISSN(Online) 2093-7423

An Effective Control Scheme of a Back-to-Back Converter with Shunt-Connected HTS SMES for Frequency Regulation of an Islanded Microgrid

Minh-Chau Dinh*, Minwon Park*, Gyeong-Hun Kim and In-Keun Yu†**

Abstract – High temperature superconducting magnetic energy storage (HTS SMES) is known as an effective solution to significantly decrease the voltage and power fluctuations of grid connected wind power generation system (WPGS). This paper implements an effective control scheme of a back-to-back converter with shunt-connected HTS SMES for the frequency regulation of an islanded microgrid. The back-to-back converter is used to connect the WPGS to the grid. A large-scale HTS SMES is linked to the DC side of the back-to-back converter through a two-quadrant DC/DC chopper. An adaptive control strategy is implemented for the back-to-back converter and the two-quadrant DC/DC chopper to improve the efficiency of the whole system. The performance of the proposed control system was evaluated in a test power system using PSCAD/EMTDC. The simulation results clearly show that the back-to-back converter with shunt-connected HTS SMES operates effectively with the proposed control strategy for stabilizing the power system frequency fluctuations.

Keywords: Energy storage system, HTS SMES, Islanded microgrid, Wind power generation system

1. Introduction

The conventional power systems are changing globally, and a large number of dispersed generation units, such as wind turbines, photovoltaic (PV) generators, fuel cells, small hydro, and wave generators, are being integrated into power systems at the distribution level. Among the renewable energy sources, the wind power generation system (WPGS) is the fastest growing. However, the WPGS output power fluctuates due to wind speed variations. This may cause some serious problems with respect to frequency and voltage oscillations when a large number of wind power generators are connected to the grid system [1-3].

To overcome these shortcomings, the smoothing control of the wind power generator output is very important. In the case of an existing microgrid, an energy storage system such as a battery energy storage system (BESS), an electric double layer capacitor (EDLC) or a superconducting magnetic energy storage (SMES) is mainly used for compensating the fluctuation of output power. Among them, high temperature superconducting magnetic energy storage (HTS SMES) has been reported as an effective solution to compensate for the fluctuations of generated power at common coupling points of the WPGS [4].

This paper discusses an effective application scheme of a back-to-back converter with shunt-connected HTS SMES for frequency stabilization within the utility regulation limits [5, 6]. An adaptive controller was designed for the back-to-back converter to improve the performance of whole system. The current controlled technique is the most essential in design application of the back-to-back converter with shunt-connected HTS SMES, because it can dominate the performance of WPGS connected to the grid system. Conventionally, the PI controllers are very common in the control of the back-to-back converter due to their simple and good performance in a wide range of operating conditions. However, they cannot always effectively control systems with changing parameters or strong nonlinearities, and they may need frequent online returning of their parameters [7]. In addition, the fuzzy logic controller shows the potential to provide an improved method even in the wide parameter variation [8]. Hence, in this paper the conventional PI controller was replaced by a fuzzy-PI controller. Then, the authors analyzed the frequency variation of a grid-connected wind power generation system using PSCAD/EMTDC (Power System Computer Aided Design/Electromagnetic Transient Including DC).

For these purposes, a large-scale HTS SMES is needed; however, the time response should be considered for practical application to the power system, in which the high speed compensation property of SMES is required. Compared to a single magnet SMES, a dual magnet SMES can ensure both high power and speed, as the operating range of the dual magnet SMES is larger than that of the single magnet, even though they have the same capacity [9]. Furthermore, the control speed of a power conditioning

† Corresponding Author: Dept. of Electrical Engineering, Changwon National University, Korea. (yuik@cwnu.ac.kr)
* Dept. of Electrical Engineering, Changwon National University, Korea. (thanchau7787@gmail.com, paku@cwnu.ac.kr)
** Korea Electrotechnology Research Institute, Korea. (kgh1001@keri.re.kr)
Received: February 12, 2014; Accepted: March 7, 2014

system (PCS) that handles the power transfer between the SMES and AC system also affects the time response of the whole system, and the back-to-back and two-quadrant DC/DC converters with an adaptive control strategy can improve the system's efficiency.

The effectiveness of the back-to-back converter with shunt-connected HTS SMES for the frequency regulation was verified. The operating characteristics of the dual magnet SMES were analyzed using PSCAD/EMTDC and the simulation results are discussed in detail.

2. Modeling of the Ulleung Island Power Network

2.1. Ulleung power network

As shown in Fig. 1, the power network of Ulleung Island consists of two diesel generators (DG), two hydraulic generators (HG), and a WPGS. The WPGS is connected to the utility through a back-to-back converter and a common wye-delta transformer. An SMES is connected to the DC side of the back-to-back converter via a DC-DC chopper.

The permanent magnet synchronous generator (PMSG) type WPGS was applied and the parameters for the wind turbine model are given in Table 1. The MOD-2 was used for the wind turbine modeling using PSCAD/EMTDC [10, 11]. In the case of PMSG, the maximum power point tracking (MPPT) control from the wind turbine was adopted. The maximum power of the wind turbine is given by Eq. (1).

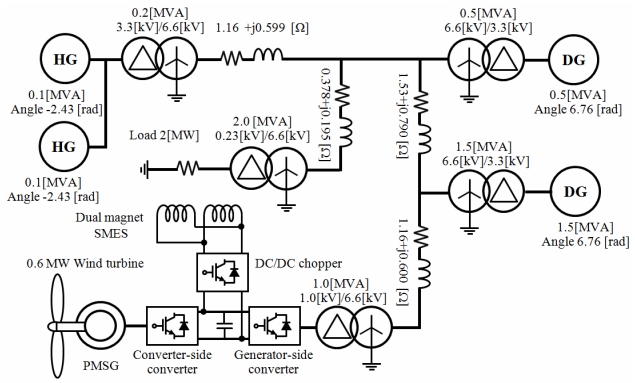

Fig. 1. The power network of Ulleung Island

Table 1. Parameters for the wind turbine model

Parameters	Values
Rated power	0.6 MW
Blade radius	24 m
Air density	1.225 kg/m^3
Rated wind speed	10.5 m/s
Rated rotation speed	3.54 rad/s
Maximum power coefficient	0.48
Optimum tip speed ratio	8.1
Inertia	731,212 Kgm^2

Table 2. Specifications of the dual magnet SMES

Parameters	Per dual magnet
Inductance	7.5 H
Critical current @20K	1.553 kA
Max. perpendicular magnetic field	21.4 gauss
Stored energy	4.43 MJ
Power capacity	0.2 MVA
Rated current	1.087 kA

$$P_{\max} = \frac{1}{2}\frac{\rho\pi R^5 C_{p\_\max}(\lambda,\beta)}{\lambda_{opt}^3}\omega_{opt}^3 \quad (1)$$

where R is the blade radius (m), C_p is the power coefficient of the wind turbine, λ is the tip speed ratio, β is the pitch angle (deg), and ω is the mechanical angular velocity of the blade (rad/s). The pitch angle control was also applied in the modeled wind turbine to limit the output power at the terminal of the generator when the wind speed was greater than the rated speed.

The capacity of SMES is strongly related to the capacity of WPGS and the features of utility. The HTS SMES as depicted in Table 2 was modeled for application to the proposed system.

2.2. Adaptive control design of the back-to-back converter with shunt-connected SMES

The control block diagram of converters is depicted in Fig. 2. The generator-side converter extracts the maximum power from the wind turbine by controlling the active power, based on Eq. (1), and controls the active power to zero. Fig. 3 represents the control block diagram of the generator-side converter. In this control strategy, the control system based on the d-q rotating reference frame is adopted.

The grid-side converter controls the DC-link voltage. By compensating the reactive power from the grid, the AC bus voltage can also be controlled. Fig. 4 shows the control block diagram of the grid-side controller system. The DC voltage and the AC bus voltage are controlled separately by the q-axis current (I_q) and d-axis current (I_d), respectively. For the d-axis and q-axis current loop regulations, the Fuzzy-PI controllers are applied [12, 13].

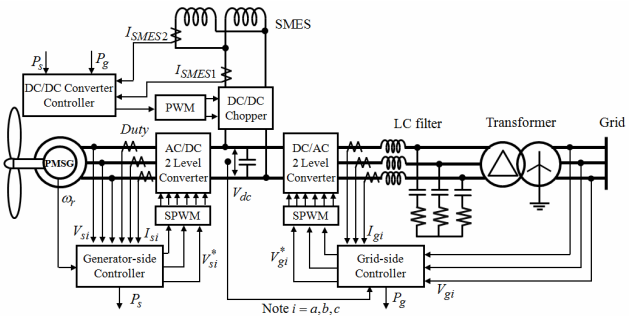

Fig. 2. The control block diagram of converters

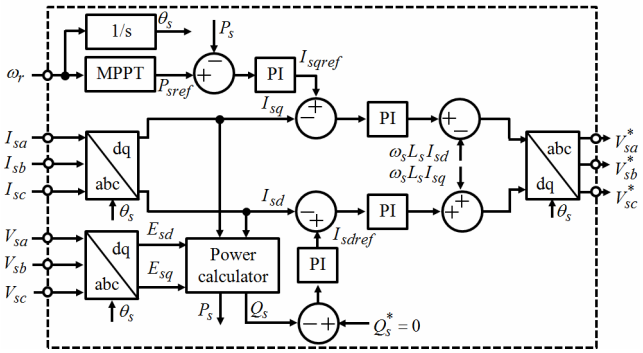

Fig. 3. The control block diagram of the generator-side controller system

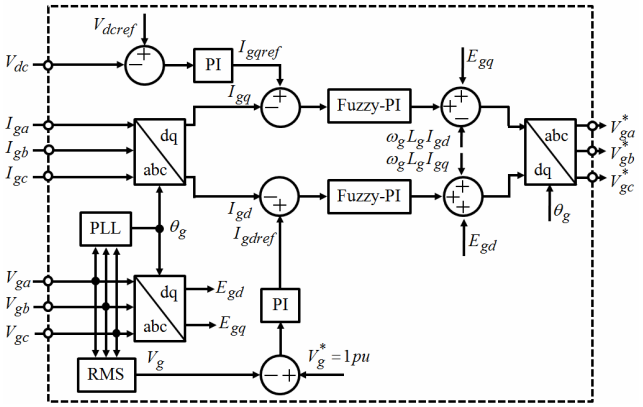

Fig. 4. The control block diagram of the grid-side controller system

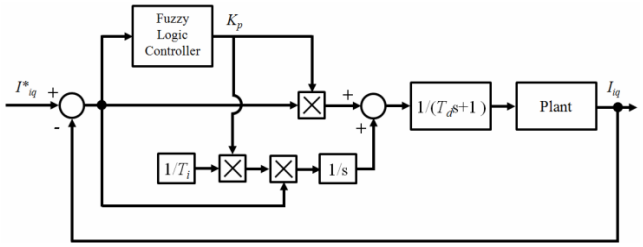

Fig. 5. Current control loop with fuzzy-PI controller

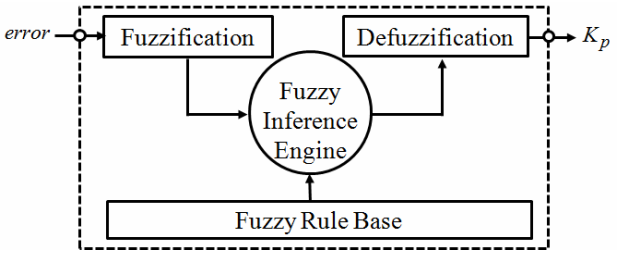

Fig. 6. The general structure of fuzzy logic control

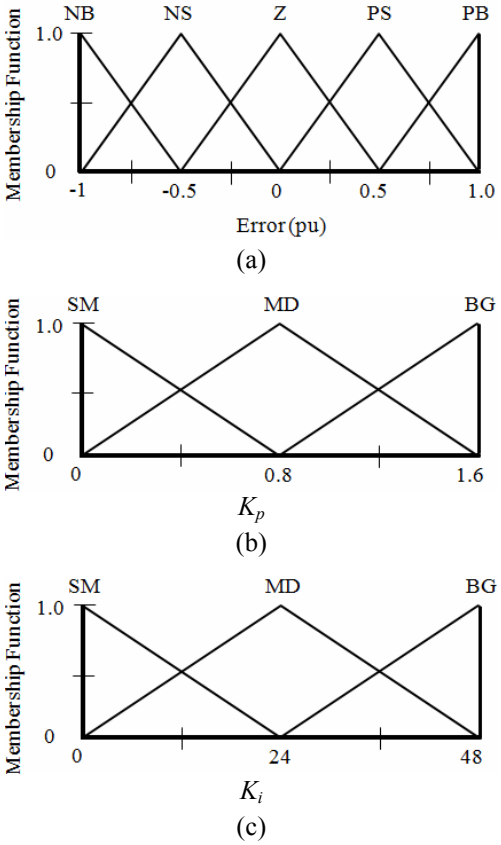

Fig. 7. (a) The membership function for the input (*error*); (b) the membership function for the output (K_p), and (c) the membership function for the output (K_i)

Fig. 5 provides a block diagram of the current control loop for the grid-side converter. The controller is composed of a Fuzzy-PI controller, a processing delay, and the plant system.

The fuzzy logic controller (FLC) is used to adjust the PI parameters including the proportional gain (K_p), the integral time constant (T_i) or the integral gain (K_i) according to the input signal error (*error*). The integral time constant (T_i) is set equal to the plan system time constant (L_{tot}/R_{tot}). L_{tot} is the total of the inductances of the LC filter and transformer. And R_{tot} is their parasitic resistances. The integral gain (K_i) is set equal to the ratio of the proportional gain and the integral time constant (K_p/T_i). To determine the proportional gain (K_p) and the integral gain (K_i), inference engine with rule base having if-then rules in the form of "If *error,* then K_p and K_i " is used.

The general structure of fuzzy logic control is shown in Fig. 6. The FLC consists of fuzzification, membership function, rule base, fuzzy inference and defuzzification.

For fuzzification of three variables of the FLC, the error (*error*) has five triangle membership functions, and the gain outputs K_p and K_i have three triangle membership functions for each gain. The variables' fuzzy subsets for inputs are Negative Big (NB), Negative Small (NS), Zero (ZE), Positive Small (PS), and Positive Big (PB). The variables' fuzzy subsets for output are Small (SM), Medium (MD), and Big (BG).

Fig. 7 (a) shows the membership function for the input (*error*). The interval input of the membership function is set at [-1 to 1] due to the variation of the d-axis or q-axis

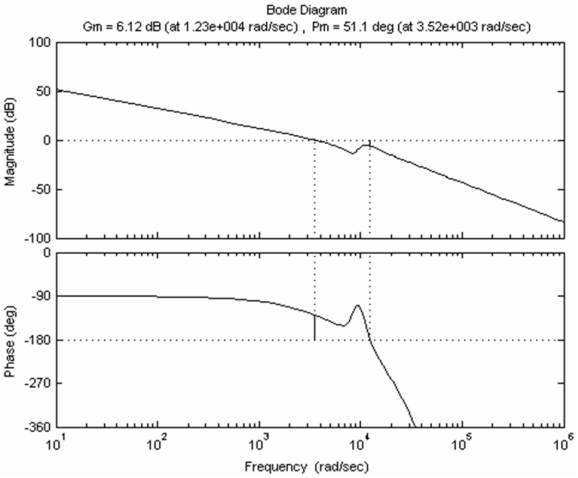

Fig. 8. Bode diagram of the current loop of the grid-side converter

current between -1 to 1 pu. Fig. 7 (b) shows the membership functions for output gain K_p. Fig. 7 (c) shows the membership functions for output gain K_i. The membership functions are designed on the basic of the frequency response of the Bode diagram of the current control loop.

Fig. 8 shows the frequency response of the Bode diagram of the current loop control. A maximum gain with gain margin (*Gm*) larger than 6 dB and phase margin (*Pm*) larger than 45 deg is obtained with K_p = 1.6 and K_i = 48. Therefore, the interval of the membership function for output gain K_p can be set at [0.0 to 1.6] as shown in Fig. 7 (b) and the interval of the membership function for output gain K_i can be set at [0.0 to 48.0] as shown in Fig. 7 (c).

The gain values of K_p and K_i for the PI controller of the current regulator are calculated for the changes in the input of the FLC according to the rule base. The rule base includes five rules as follows:

If (*error* is NB), then (K_p is BG) and (K_i is BG)
If (*error* is NS), then (K_p is MD) and (K_i is MD)
If (*error* is Z), then (K_p is SM) and (K_i is SM)
If (*error* is PS), then (K_p is MD) and (K_i is MD)
If (*error* is PB), then (K_p is BG) and (K_i is BG)

In this paper, the inference mechanism utilizes Mamdani's max-min method. In the defuzzification, the output fuzzy system is a weighted average of the outputs for all rules. The solution to the defuzzification process is computed by the following equation:

$$K_p = \frac{\sum_{i=1}^{n} \mu_i Y_i}{\sum_{i=1}^{n} \mu_i} \tag{2}$$

where n is the number of rules, μ_i is the degree of the membership function for the i^{th} rule, and Y_i is the consequence membership function. The PSCAD/EMTDC software does not include a component for FLC. Therefore, the authors developed a new FLC component for Fuzzy-PI in PSCAD / EMTDC by using FORTRAN codes. The detailed parameters of the back-to-back converter system are summarized in Table 3.

Table 3. Detailed parameters of the back-to-back converter

Components	Parameters	Values
Back-to-back converter	Switching frequency	5 kHz
	Grid frequency	60 Hz
	DC-link capacitor	25,000 μF
	DC-link voltage	2.0 kV
LC filter	Inverter side inductance	0.065 pu
	Inverter side parasitic resistance	0.0056 pu
	Filter capacitor	0.05 pu
	Damping capacitor	0.3 pu
Step up transformer	Transformer inductance	0.04 pu
	Transformer resistance	0.015 pu
	Low voltage	1.2 kV
	High voltage	6.6 kV

3. Frequency Regulation by the SMES System

The grid frequency has to be regulated within the utility regulation limits of 60 ± 0.2 Hz. The control block diagram shown in Fig. 9 was used for the frequency stabilizations. If both E_{SMES1} and E_{SMES2} are in the range of 0 pu to 1 pu, the *control* is active (0); otherwise, it is controlled (1). If *control* is one, the DC/DC chopper does not charge or discharge energy to the SMES.

When the *control* is zero, the output power of WPGS (P_s) is fed to a low-pass filter and then compared with output power of the back-to-back converter (P_g) to control

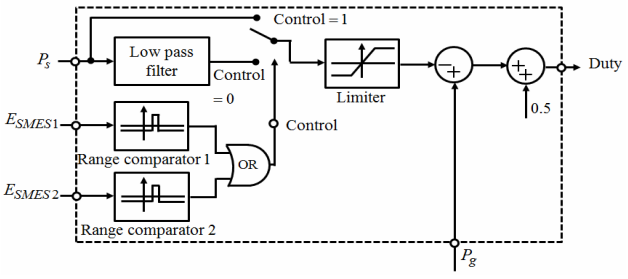

Fig. 9. Control block diagram of the dual magnet SMES

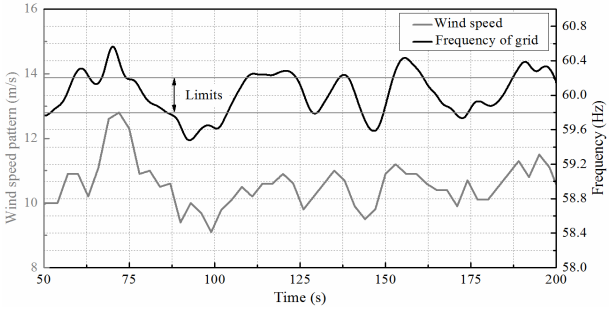

Fig. 10. Wind speed pattern of WPGS and frequency variations of Ulleung Island power network

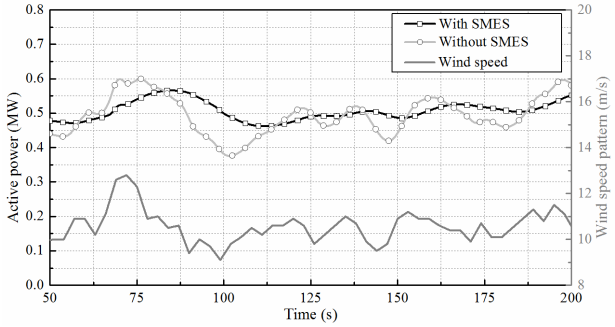

Fig. 11. Comparison results of feeding active power to the grid of WPGS in the cases with and without the HTS SMES

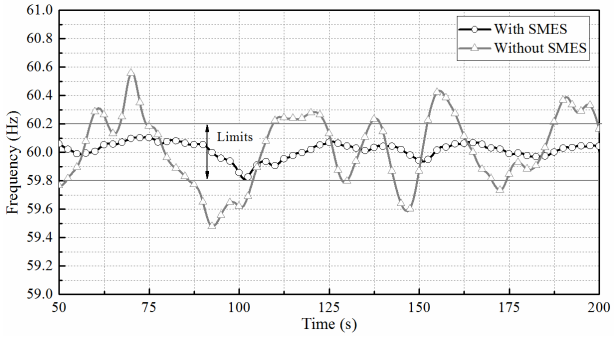

Fig. 12. Grid frequency when the SMES is applied

the duty of the DC/DC chopper.

The controller provides the switching control signal for the DC/DC chopper. Fig. 10 reports the wind speed pattern and grid frequency variations without the SMES system. The frequency of the model power system exceeds the regulations limit of 60 ± 0.2 Hz. As shown in Fig. 11, the output power of the PMSG type WPGS in combination with the HTS SMES fluctuates much less than that of the general PMSG type WPGS under the same wind speed. The results in Fig. 12 verify that the grid frequency is maintained in the range of 59.8 Hz to 60.2 Hz when the SMES is applied.

4. Conclusion

This paper dealt with the frequency stabilization of the Ulleung Island power network by an effective control scheme of the back-to-back converter with shunt-connected HTS SMES. For these purposes, a control system including the adaptive controller of the grid-side converter was designed and applied to the back-to-back and DC-DC converters. From the simulation results, it can clearly be concluded that the proposed system properly regulates the frequency within the regulation limits. Compared to the general configurations of SMES system, the back-to-back converter with shunt-connected SMES can save one converter and also reduce the power losses of converter system. Hence, the proposed system is cost-effective in comparison with the general WPGS and SMES system.

Acknowledgements

This research is financially supported by Changwon National University in 2013-2014

References

[1] B. Bladberg *et al.*, "Power electronics as efficient interface in dispersed power generation systems," *IEEE Trans. Power Electronics*, vol. 19, pp. 1184-1194, Sept. 2004.

[2] R.D. Fernández, P.E. Battaiotto, R.J. Mantz, "Wind farm non-linear control for damping electromechanical oscillations of power systems," *Renew. Energy, 33 (2008)*, pp. 2258.

[3] Narchi Linn, Yushi Miura, and Toshifumi, "Power system stabilization control by HVDC with SMES using virtual synchronous generator," *IEEJ Journal of Industry Applications*, Vol. 1, No. 2, pp. 102-110, March 27, 2012.

[4] Mohd. Hasan Ali, Bin Wu, and Roger A. Dougal, "An overview of SMES application in power and energy systems," *IEEE Transactions on Sustainable Energy,* Vol. 1, No. 1, April 2010.

[5] M. Stephen et al., "Power quality solutions for semiconductor tools," *Power Quality Assurance,* pp. 24-31, May/June 2010.

[6] H. Y. Yung et al., "A study on the operating characteristics of SMES for the dispersed power generation system," *IEEE. Trans. Applied Superconductivity*, vol. 19, no. 3, pp. 2028-2031, 2009.

[7] B. Ferdi, C. Benachaiba, S. Dib, R. Dehini, "Adaptive PI control of dynamic voltage restorer using fuzzy logic," *Journal of Electrical Engineering: Theory and Application,* Vol. 1, pp. 165-173, 2010.

[8] M. Rukonuzzaman, M. Nakaoka, "Fuzzy logic current controller for three-phase voltage source PWM-inverters," *Industry Application Conference,* Vol. 2, pp. 1163-1169, 2000.

[9] A-Rong Kim et al., "Operating characteristic analysis of HTS SMES for frequency stabilization of dispersed power Generation System," *IEEE Trans. Applie. Supercond,* Vol. 20, pp. 1334-138, June 2012.

[10] Thanh Hai Nguyen and Dong-Choon Lee, "Ride-through technique for PMSG wind turbines using energy storage system," *Journal of Power Electronics*, Vol. 10, No. 6, November 2010.

[11] G. H. Kim, A. R. Kim, S. Kim, M. Park, I. K. Yu, K. C. Seong, and Y.J. Won, "A novel HTS SMES application in combination with a permanent magnet synchronous generator type wind power generation

system," *Physica C: Superconductivity,* vol. 471, issues 21-22, pp. 1413-1418, November 2011.
[12] Ahmet Teke, M. Emin Meral, Lutfu Sarubulut and Mehmet Tumay, "Implementation of fuzzy logic controller using Fortran language in PSCAD/ EMTDC," *International Journal of Electrical Engi-neering,* Vol. 48, Issue 4, pp. 372, Oct 2011.
[13] Marwan Rosyadi, S. M. Muyeen, Rion Takahashi, and Junji Tamura, "Fuzzy logic controlled voltage source converter in grid connected application via LCL filter," *Electrical Machines and Systems (ICEMS),* 21-24 Oct. 2012.

Minh-Chau Dinh He received the B.S. degree from Hanoi University of Science and Technology, Hanoi, Vietnam, in 2010 and the M.S. degree from Changwon National University, Changwon, Korea, in 2012, all in electrical engineering. He is currently working toward the Ph.D. degree in electrical engineering at Changwon National University, Changwon, Korea. His fields of interest are high voltage direct current system and superconducting power cable.

Minwon Park He received B.S degree in Electrical Engineering from Changwon National University in 1997 and his M.S. and Ph.D. degrees in Electrical Engineering from Osaka University in 2000 and 2002, respectively. His research interests are the development of the simulation model of power conversion equipment and renewable energy sources using EMTP type Simulators.

Gyeong-Hun Kim He received his B.S., M.S., and Ph.D. degrees in Electrical Engineering from Changwon National University, Korea in 2007, 2009, and 2013, respectively. He has been with the Korea Electrotechnology Research Institute (KERI), Changwon, Korea, since 2013. Currently, he is a senior research engineer with the Smart Distribution Research Center, KERI. His research interests are operation and control of a wind power generation system.

In-Keun Yu He received B.S degree in Electrical Engineering from Dongguk University in 1981 and his M.S. and Ph.D. degrees in Electrical Engineering from Hanyang University in 1983 and 1986, respectively. His research interests are electric energy storage and control systems, PSCAD/EMTDC and RTDS simulation studies, and renewable energy sources.